CALCULATION OF MECHANICAL, THERMODYNAMIC AND TRANSPORT PROPERTIES OF METALLIC GLASS FORMERS

Tahir Çağın,[a,*] Yoshitaka Kimura,[a] Yue Qi,[a] Hao Li,[a] Hideyuki Ikeda,[a,b]
William L. Johnson[b] and William A. Goddard, III[a,*]

a) Materials and Process Simulation Center, 139-74
California Institute of Technology, Pasadena, CA 91125, U.S.A.

b) Materials Science Department,
California Institute of Technology, Pasadena, CA 91125, U.S.A.

Abstract

Recently, we have parametrized Sutton-Chen type empirical many body force fields for FCC transition metals to study the thermodynamic, mechanical, transport and phase behavior of metals and their alloys. We have utilized these potentials in lattice dynamics calculations and molecular dynamics simulations to describe the structure, thermodynamic, mechanical and transport properties of pure metals and binary alloys in solid, liquid and glass phases. Here, we will describe these applications: mechanical properties of binary alloys $(Pt - Rh)$ and viscosity of a binary alloy, $(Au - Cu)$, as a function of composition, temperature, and shear rate, crystal-liquid, liquid-crystal phase transformation in $(Ni - Cu)$, liquid to glass transformation in a model glass former, $(Ag - Cu)$.

1 Introduction

The development of advanced high performance materials in industrial world is increasingly coupled with the theoretical and computational modeling. In this process focus is on research areas having direct impact on innovative development of such materials. The high performance metalic alloys find use in various segments of materials and chemical industry as catalysts, low weight and high strength structural materials. The theory and computational efforts require and strive for i) *a priori* determination of the ultimate properties of metals, metallic alloys, ii) simulation and modeling of the processing conditions, iii) investigating the performance characteristics of these metals and alloys. All these are extremely important for timely, cost efficient and environmentally compliant development of such advanced materials. With the advances in computational speed and the emerging new computational algorithms, the theory and computer simulations are positioned in the midst of this innovative process.

Understanding the kinetics and thermodynamics of supercooled bulk metallic glass forming liquids is of critical importance in developing light weight high-performance amorphous metallic glasses [1]. Especially, determination of viscosity as a function of temperature and concentration and microscopic level studies on the kinetics of crystallization and glass formation are amenable through computer simulations. Here, we applied these new FF parameters in MD simulation of metals and alloys to

1. determine the mechanical properties (eg. elastic constants of Pt-Rh alloy as a function of concetration and temperature)

2. determine the shear viscosity of Au:Cu binary alloys as a function of temperature and concentration from nonequilibrium molecular dynamics (NEMD).

3. study the role of atomic size in crystalization and glass formation processes in metallic alloys from equilibrium molecular dynamics (EMD).

In the next section we present the parameters used in metal and alloy simulations. Subsequently, we will describe the three applications.

Mat. Res. Soc. Symp. Proc. Vol. 554 © 1999 Materials Research Society

Table 1: Parameters sets for the Quantum Sutton-Chen many-body potential for fcc transition metals.

	n	m	$D(eV)$	c	$\alpha(\AA)$
Ni	10	5	7.3767E-3	84.745	3.5157
Cu	10	5	5.7921E-3	84.843	3.6030
Rh	13	5	2.4612E-3	305.499	3.7984
Pd	12	6	3.2864E-3	148.205	3.8813
Ag	11	6	3.9450E-3	96.524	4.0691
Ir	13	6	3.7674E-3	224.815	3.8344
Pt	11	7	9.7894E-3	71.336	3.9163
Au	11	8	7.8052E-3	53.581	4.0651

2 Parameters for FCC transition metals

Computer simulations on various model systems usually use simple pair potentials. On many occasions to account for the directionality of bonding three body interactions were also employed. But, the interactions in metals and metal alloys can not be represented by simple pairwise interactions. In these systems the electron density plays a dominant role in interactions and resulting physical properties. Therefore interactions in metals and metal alloys are dominated by the many-body interactions. In simple sp-bonded metals this effect may be represented by the interaction potentials derived from model pseudopotentials using the second order perturbation theory [2]. However,for d-band metal and metal alloys the model pseudopotential approach gives way to newer techniques evolved over the past ten years to account for the many body effects. Among these approaches we can list the empirical many body potentials based on Norskov's Effective Medium Theory [3], Daw and Baskes' Embedded Atom Method [4], Finnis and Sinclair's [5] empirical many body potentials, and more recently the many body potentials developed by Sutton and co-workers [6,7] within the context of tight binding approach [8].

We adopted the Sutton-Chen form, where the total potential energy of the metal is given by Eq. (1)

$$U_{tot} = \sum_i U_i = \sum_i \epsilon \left[\sum_{j \neq i} \frac{1}{2} V(r_{ij}) - c\rho_i^{1/2} \right] \tag{1}$$

Here $V(r_{ij})$ is a pair potential defined by Eq. (2);

$$V(r_{ij}) = \left(\frac{a}{r_{ij}} \right)^n \tag{2}$$

accounting for the repulsion (Pauli orthogonality) between the i and j atomic cores and ρ_i is a local density accounting for cohesion associated with atom i defined by Eq. (3);

$$\rho_i = \sum_{j \neq i} \phi(r_{ij}) = \sum_{j \neq i} \left(\frac{a}{r_{ij}} \right)^m \tag{3}$$

In Eqs. (1)-(3), r_{ij} is the distance between atoms i and j, a is a length parameter scaling all spacings (leading to dimensionless V and ρ), c is a dimensionless parameter scaling the attractive terms, ϵ sets the overall energy scale, and n, m are integer parameters such that $n > m$. [The interaction cut-off range in (1) and (3) is chosen to be twice the lattice parameter of the fundamental cubic unit cell.] Given the exponents (n,m), c is determined by the equilibrium lattice parameter and ϵ is determined by the total cohesive energy (E_{coh}). The parameters for transition metals, Ni, Cu,Rh, Pd, Ag, Ir, Au, Pt are given in Table 1.

To simulate alloys, we use the following combination rules to represent the interaction between A-B pairs

$$D_{ij} = \sqrt{D_i D_j} \qquad m_{ij} = \frac{(m_i + m_j)}{2} \qquad n_{ij} = \frac{(n_i + n_j)}{2} \qquad \alpha_{ij} = \frac{(\alpha_i + \alpha_j)}{2} \tag{4}$$

3 Applications

3.1 Elastic constants of Pt-Rh alloy at elevated temperatures

We used MD simulations to calculate the elastic properties of metals and alloys. As an example here we present the results for Pt-Rh alloy simulated at various temperatures by varying the concentration.

In our computations at each concentration and at each temperature, first the zero strain state, h_o, of the system is determined by performing constant temperature and constant stress simulations (NPT) at zero stress. This yields the reference shape and size matrix, h_o in Parrinello-Rahman formalism [9]. In determining elastic constants this reference state is used in constant temperature constant volume simulations (NVE) of 50000 steps for each state point. The elastic constants are evaluated using the following statistical fluctuation formulas

$$\begin{aligned} C^T_{ijkl} &= -\frac{\Omega_o}{k_B T}(< P_{ij}P_{kl} > - < P_{ij} >< P_{kl} >) \\ &\quad + \frac{2Nk_BT(\delta_{ik}\delta_{jl} + \delta_{il}\delta_{jk})}{\Omega_o} + < \chi_{ijkl} > \end{aligned} \tag{5}$$

where <> denotes the averaging over time and $\Omega_o = deth_o$ is the reference volume for the model system. The first term represents the contribution from the fluctuation of the microscopic stress tensor, P_{ij}, the second term represents the kinetic energy contribution, and the third term is the Born term.

After equilibration of 20,000 steps (20 ps with a time step of 1 fs) we calculated the elastic constants at 6 different concentrations, 0, 20, 40 ,60, and 100 % at 300 K after collecting statistics over 50,000 steps for the fluctuation terms. As reported eariler the botn terms converges within first few 1000 steps. The results are given in Table 2.

Table:2 Elastic constants and bulk modulus of Pt-Rh binary alloy calculated at 300^0K as obtained from NVE MD Simulation after 50000 steps.

Percent Rh @ Pt	C_{11} (GPa)	C_{12} (GPa)	C_{44} (GPa)	B (GPa)
0	253.4 ±1.3	208.1±0.5	60.1 ±0.2	223.4 ±0.8
20	268.4 ±0.4	213.8 ±1.0	73.4 ±0.9	232.3 ±0.8
40	282.2 ±0.3	216.2 ±0.3	88.1 ±0.5	238.0 ±0.3
60	289.1 ±1.2	212.6 ±0.8	101.8 ±1.0	237.3 ±0.9
80	298.1 ±0.4	211.9 ±0.3	114.0 ±0.6	240.5 ±0.4
100	303.5 ±0.4	208.5 ±0.4	125.1 ±0.2	240.4 ±0.4

3.2 Shear viscosity of metals and alloys

Using Nonequilibrium molecular dynamics (NEMD) methods, we calculated the shear viscosity of Cu-Au alloys subjected to a planar Couette shear flow. We used the parameters given in Table 1 above. These parameters are shown to give accurate values for surface energies, vacancies energies, and stacking faults.

We considered temperatures of 1500K, 1750K, and 2000K and alloys $Au_x - Cu_{1-x}$ with $x = 0$, 0.25, 0.5, 0.75, and 1.0. The NEMD simulation used periodic boundary conditions with (500 atoms per cubic unit cell). The unit cell length was based on extroplating the experimental density at the corresponding temperature. For alloys we assumed that the density is given by the linear combination rule

$$\rho_T\left(Au_xCu_{1-x}\right) = \rho_T\left(Au\right)\cdot x + \rho_T\left(Cu\right)\cdot(1-x)$$

We applied shear rates of $\dot{\gamma} = 2$, 1, 0.5, and 0.25 ps^{-1}. For each shear rate and temperature, we first equilibrated (with NEMD) for N_{EQ} steps followed by $N_{meas} = 9N_{EQ}$ steps which were used to calculate properties. As the shear rate decreases we observed larger fluctuations and slower convergence. Thus, we increased the number of steps. The total number of steps ranged from 20,000 ($\dot{\gamma} = 2$) to 100,000 ($\dot{\gamma} = 0.25$). The calculated viscosity scaled as $\dot{\gamma}$ as shown in Figure 1. This relation was used to extrapolate the $\dot{\gamma} = 0$ for comparison to experiment. The results are summarized in Table 3. The calculations are within 1 to 3 %

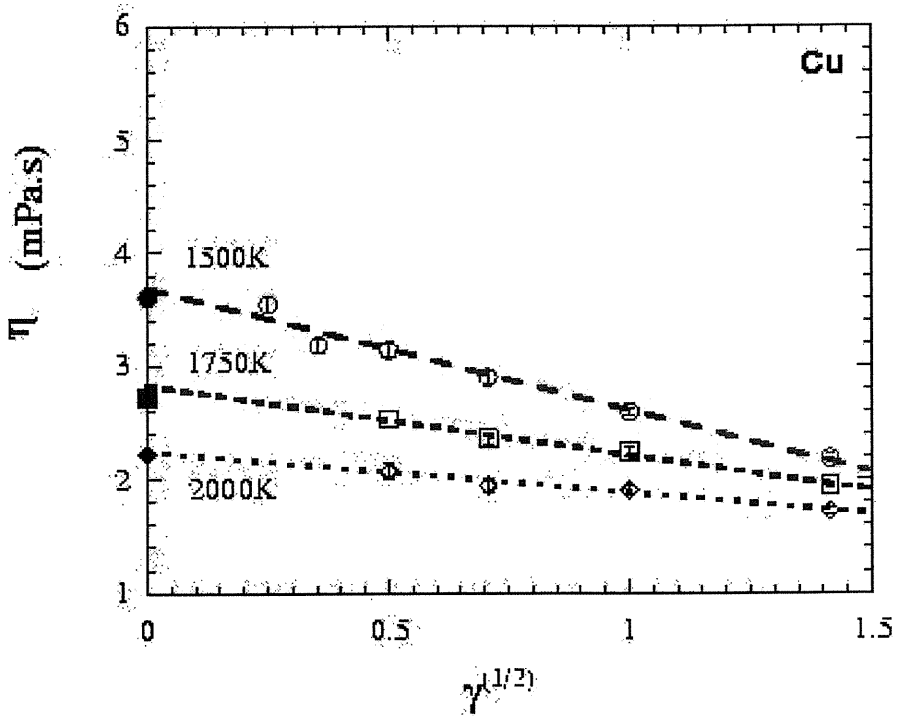

Figure 1: Viscosity as a function of shear rate.

for Cu but high by 12 to 30 % for Au. These exploration calculations will be extended next year by using much slower rates and by considering NPT MD rather than NVT MD.

Table:3 Viscosity at zero shear rate, η_0 (mPas).

T (K)	Cu Sim.	Cu Exper.	Cu_3Au_1 Sim.	Cu_1Au_1 Sim.	Cu_1Au_3 Sim.	Au Sim.	Au Exper.
1500	3.68	3.6	2.64	2.88	3.97	5.86	4.5
1750	2.82	2.72	2.29	2.47	3.21	4.56	3.7
2000	2.24	2.22	1.87	2.04	2.70	3.67	3.2

3.3 Glass formation and Crystallization in metals and alloys

In this section, we use molecular dynamics to examine melting and quenching of CuNi and CuAg alloys. These two model systems were particularly chosen, since Cu and Ag have very different sizes, making them good candidates for forming a metal glass, while Cu and Ni have similar sizes thus making them good candidates for forming a crystal even at high quenching rates.

The simulations in this section performed in constant temperature, constant thermodynamic tension (TtN) MD conditions [10]. The TtN MD simulations started from a cubic box with 500 atoms subject to periodic boundary conditions. To obtain the stress free reference size and shape of the unit cell, we performed 25 ps of simulation with constant enthalpy, constant thermodynamic tension (HtN) at zero pressure. The TtN MD simulations were carried out in a series of increasing temperatures from 300 to 1500K in 100K increments. The final temperature of 1500K is a few hundred degrees above the melting temperature. At every temperature the MD time step was taken as 1 fs and the simulation time for determining the properties was 25 ps.

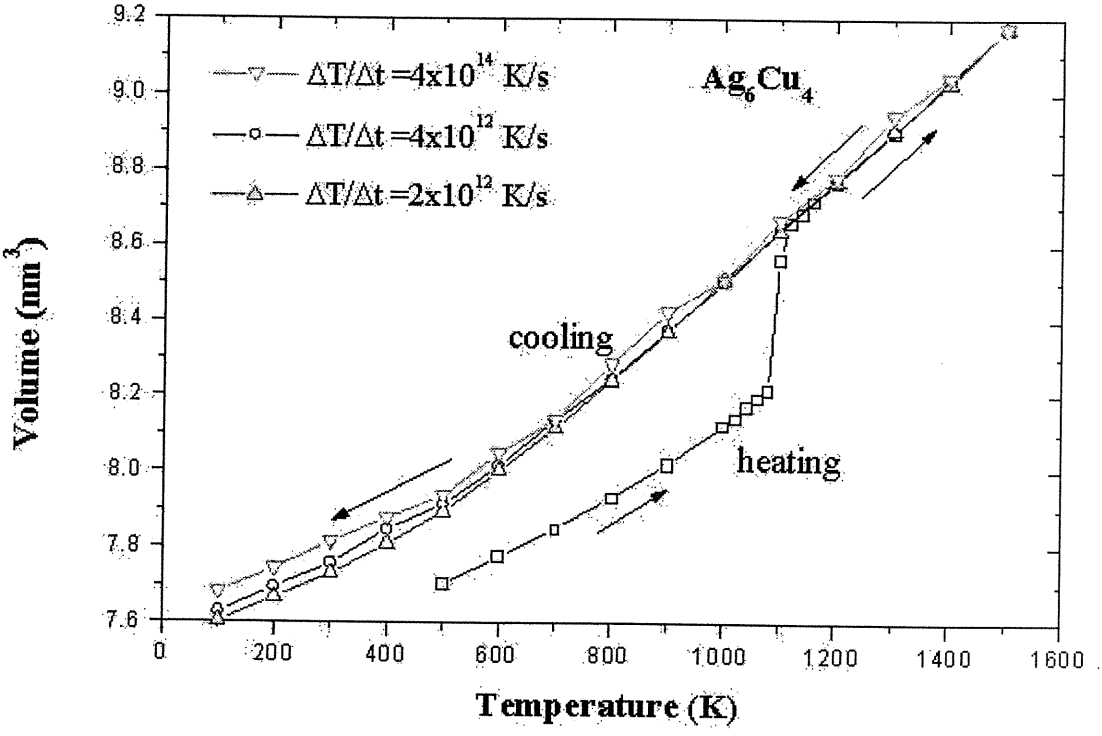

Figure 2: Ag-Cu alloy at the eutectic composition.

After equilibrating the structure in the liquid phase at 1500K, we cooled the system using different quenching rates from 1500K down to 300K in 100K decrements in the TtN ensemble. To achieve the fast, intermediate, and slow cooling rates, we kept the model system at the same temperature for times of 50 ps, 25 ps, and 0.25 ps. This leads to cooling rates of 2×10^{12}, 4×10^{12}, and 4×10^{14} K/s, respectively. To ensure convergence of the results for the fastest cooling rate (0.25 ps per 100K), using the conditions at the end of each 0.25 ps interval (for each 100 K drop) we performed additional 25 ps long TtN simulations for thermodynamic averaging.

Figure 2 shows the variation of the volume as Ag_6Cu_4 is heated and cooled. The large jump in volume in the temperature range of 1000K to 1200K for the heating process is due to the melting of the Ag-Cu alloy. In order to obtain a more refined estimate of T_{melt}, we used a smaller increment in temperature, namely 20K, from 1000K to 1200K. This leads to a theoretical melting temperature, $T_{melt} = 1090$K, in reasonable agreement with experimental melting temperature of 1053K. One reason for the melting temperature being a bit high is that our system is homogeneous without a free surface. In addition, we started with a perfect crystal; given the rapid rate of heating, the system might not have had time to generate an equilibrium distribution of defects, thus leading to a slightly higher T_{melt}.

Using cooling rates in the range of 2×10^{12} to 4×10^{14} K/s, we find that CuNi and pure Cu always form a face-centered cubic (fcc) crystal while Cu_4Ag_6 always forms a glass (with T_g decreasing as the quench rate increases). The crystal formers have radius ratios of 1.025 (CuNi) and 1.00 (Cu) while the glass former (CuAg) has a ratio of 1.13, confirming the role of size mismatch in biasing toward glass formation.

We have considered several cooling rates to investigate its effect on the glass transition temperature T_g. Each rate leads to a slightly different value for the temperature at which the slope changes. A parameter often used to define the glass transition temperature is the Wendt-Abraham parameter [11] defined by $R = g_{min}/g_{max}$. Here $g_{min}(g_{max})$ is the value of $g(r)$ at the first minimum (maximum) in the RDF. The Wendt-Abraham parameter stresses the local character of $g(r)$, permitting a direct comparison between structures and leading to a better estimate of glass transition temperatures. The Wendt-Abraham transition temperature, T_g^{WA}, are $T_g^{WA} \approx 500$K at $\Delta T/\Delta t = 2 \cdot 10^{12}$ K/s, $T_g^{WA} \approx 550$ K at $\Delta T/dt = 4 \times 10^{12}$ K/s, and $T_g^{WA} \approx 700$ K at $\Delta T/\Delta t \approx 4 \cdot 10^{14}$ K/s. Thus, the glass transition temperature increases with

increased cooling rate. The fastest cooling rates result in shorter times for the atoms to relax, thus leading to formation of the glass at a higher temperature than at lower cooling rate.

4 Concluding Remarks

We presented a many body potential parameterized to simulate fcc transition metals and their alloys. We have used these potentails and described combination rules to study elastic properties of binary alloy Pt-Rh, to study the shear viscosity of Au-Cu binary melt and finally to study the glass formation from melt at the eutectic concentration for Ag-Cu.

Acknowldegements This research was supported partially by a grant (ARO-DAAH 95-1-0233) from the Army Research Office and by grants from the NSF (ASC 92-17368 and CHE 95-12279). In addition, support for the Materials Simulation Center (MSC) facilities came from DOE-ASCI, ARO-DURIP (DAAG55-97-1-0140), and MSC industrial associates.

References

[1] P. Duwez, R. H. Willens, and W. Klement Jr. *J. Appl. Phys.* **31**, 1137 (1960). A. Peker and W. L. Johnson *Appl. Phys. Lett.* **63** 2342 (1993); X. H. Liu and W. L. Johnson *J. Appl. Phys.* **78** 6514 (1995).

[2] W. A. Harrison, **Solid State Theory** (Dover, NY, 1979)
W. A. Harrison, **Electronic Structure and Properties of Solids** (Dover, NY, 1980)

[3] J. K. Norskov, Phys. Rev. B 26, 2875 (1982)

[4] M. S. Daw, M. L. Baskes, Phys. Rev. B 29, 6443 (1984)

[5] M. W. Finnis, J. F. Sinclair, Phil. Mag. A, 45 (1984)

[6] A. P. Sutton, J. Chen, Phil. Mag. Lett. 61, 139 (1990)

[7] H. Rafii-Tabar, A. P. Sutton, Phil. Mag. Lett. 63, 217 (1991)

[8] D. D. Koleske, S. J. Sibener, Surf. Sci. 290, 179 (1993)

[9] S. Nosè *Mol. Phys.* **52** , 255 (1984); S. Nosè *J. Chem. Phys.* **81**, 511 (1984). M. Parrinello and A. Rahman *Phys. Rev. Lett.* **45** 1196 (1980).

[10] J. R. Ray and A. Rahman *J. Chem. Phys.* **82** 4243 (1985).

[11]H. R. Wendt and F. F. Abraham *Phys. Rev. Lett.* **41** 1244 (1978).